# Efficient Topological Cleaning for Visual Colon Surface Flattening

Rui Shi[1], Wei Zeng[2], Jerome Zhengrong Liang[1], and Xianfeng David Gu[1]

[1] Department of Computer Science, Department of Radiology,
Stony Brook University, Stony Brook, NY 11794, USA
rshi@cs.sunysb.edu
[2] School of Computing & Information Sciences, Florida International University,
11200 SW 71st, Miami, FL 33199, USA

**Abstract.** Conformal mapping provides a unique way to flatten the three dimensional (3D) anatomically-complicated colon wall. Visualizing the flattened 2D colon wall supplies an alternative means for the task of detecting abnormality as compared to the conventional endoscopic views. In addition to the visualization, the flattened colon wall carries supplementary geometry and texture information for computer aided detection of abnormality. It is hypothesized that utilizing both the original 3D and the flattened 2D colon walls shall improve the detection capacity of currently available computed tomography colonography. One of the major challenges for the conformal colon flattening is how to make the input colon wall inner surface to be genus zero, as this is required by the flatten algorithm and will guarantee high flatten quality. This paper describes an efficient topological cleaning algorithm for the conformal colon flattening pipeline. Starting from a segmented colon wall, the Marching Cube algorithm was first applied to generate the surface, then we apply our topological clearance algorithm to remove the topological outliers to guarantee the output surface is exactly genus 0. The cleared or denoised colon surface was then flattened by an Ricci flow. The pipeline was tested by 14 patient datasets with comparison to our previous work.

**Keywords:** Flattening, conformal mapping, homotopy, Ricci flow, virtual colonoscopy.

## 1 Introduction

Virtual colonoscopy (VC), mimicking the conventional optical colonoscopy (OC), is a medical imaging procedure which uses X-rays or magnetic resonance (MR) signals and computers (1) to produce two and three-dimensional (3D) images of the colon (large intestine) from the lowest part, i.e., the rectum, all the way toward the lower end (i.e., the cecum) of the small intestine, and (2) to visualize the colon mucosal surface by endoscopic views on a screen [7,8]. The procedure has shown the potential to screen colonic polyps and detect colon diseases, including diverticulosis and cancer [14].

Traditional paradigm in VC employs X-ray computed tomography or computed tomography colonography (CTC) to achieve the tasks of screening and detection due to the high speed of CT scanning and high contrast between colon wall and colon lumen filled by CO2 or air in CT images. While MR colonography (MRC) has an attractive

H. Yoshida, D. Hawkes, M.W. Vannier (Eds.): Abdominal Imaging 2012, LNCS 7601, pp. 20–29, 2012.

point of non-ionization radiation [16], it faces several drawbacks, e.g., lower spatial resolution, prone to motion artifacts, and noticeable susceptibility artifacts on the interface between air and tissue/colon wall. Therefore, MRC remains in the early research development stage, while CTC has been successfully demonstrated to be more convenient and efficient than OC as a screening modality [14]. A combination of VC screening with OC follow-up for therapeutic intervention could be a cost-effective means to prevent the deadly disease of colon cancer.

However, because of the length of the colon with complicated structures, inspecting the entire colon wall is time consuming and prone to errors by current VC technologies. Moreover, because of the complicated colon structure, the field-of-view (FOV) of the VC endoscopic views is limited, resulting in incomplete examinations. Flattening the 3D wall into a 2D image would effectively increase the FOV and provide supplementary information to the VC endoscopic views [5]. Thereafter, various flattening techniques [2,3,9,13,10,18] have been developed, among which the conformal mapping algorithm [9,10] showed advantages in generating 2D colon wall image with minimal distortion by preserving the structural angles.

Paik et al. [13] used cartographic projections to project the whole solid angle of the camera. This approach samples the solid angle of the camera, and maps it onto a cylinder which is finally mapped to a 2D planar image. However, this method causes distortions in shape. Bartrol et al. [3] moved a camera along the central path of the colon. However, this approach does not provide a complete overview of the colon. Haker et al. [5] employed certain angle-preserving mappings, based on a discretization of the Laplace-Beltrami operator, to flatten a surface onto a plane in a manner which preserves the local geometry. However, the flattened result of their method is not efficient for applications like polyp identification, and it requires a highly accurate and smooth surface mesh to achieve a good mean-curvature calculation. Wang, et al. [18] explored a volume-based flattening strategy to visualize the textures of the original 3D colon wall in the flattened 2D image. However, the distance-based mapping may not be accurate enough for detection of small polyps. The associated computation is intensive.

Hong et al. [9,15] utilized conformal structure to flatten the colon wall onto a planar image. Their method is angle preserving and minimizes the global distortion. First, the colon wall is segmented and extracted from the CTC image data set. The topology noise (i.e., minute handle) is removed by a volumetric algorithm. The holomorphic 1-form, a pair of orthogonal vector fields, is then computed on the 3D colon surface mesh using the conjugate gradient method. The colon surface is cut along a vertical trajectory traced using the holomorphic 1-form. Consequently, the 3D colon surface is conformal mapped onto a 2D rectangle. The flattened 2D mesh is then rendered using a direct volume rendering method accelerated with the GPU strategy. For applications like polyp detection, the shape of the polyps is well preserved on the flattened colon images, and thus provides an efficient way to enhance the navigation of a virtual colonoscopy system.

Unfortunately, the de-noise algorithm in [9,15] cannot always get genus 0 surface (actually only one case succeed out of 14). In this paper, topological de-noise is solved by our new algorithm, which guarantees the output surface to be genus 0. This efficient de-noise algorithm greatly improved the efficiency and accuracy and deliver comparable flattening results.

## 2 Method

Fig. 1 shows our new conformal mapping pipeline with comparison to our previous one. From acquired CTC datasets, our first task was to segment each image data volume and extract the corresponding colon wall. This was achieved by a statistical maximum a posteriori expectation-maximization (MAP-EM) algorithm [17]. Both our present and previous pipelines share this task. Then a triangle mesh of the colon wall mucosal surface was generated by the standard Marching Cube algorithm. To remove topology handles, a new surface-based de-noise algorithm was applied. In our present pipeline, the Marching Cube algorithm was applied prior to topological de-noising. After de-noising, we developed Ricci flow method to perform the conformal flattening task.

Conformal mapping has many unique properties in flattening the colon wall, as shown in [9]. However, as we mentioned, the old de-noise method cannot guarantee the output surface is genus 0. Our contribution: we developed and applied a new topological de-noise algorithm, which is very efficient and can guarantee the output surface to be genus 0.

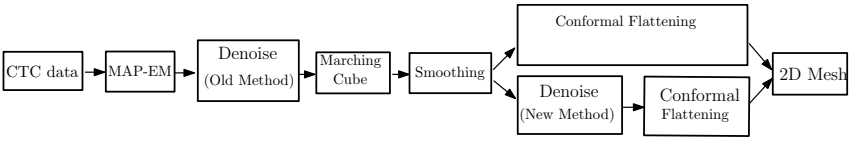


**Fig. 1.** Pipeline for our previous and current methods

## 3 Theoretic Background

This section briefly introduces elementary theories of surface topology and surface Ricci Flow.

### 3.1 Homotopy Basis

**Definition 1** ***(Homotopy).*** *Two continuous maps $f_0, f_1 : M \to N$ are said to be homotopic if there is a continuous map $f : M \times I \to N$ such that $F(\cdot,0) = f_0$ and $F(\cdot,1) = f_1$. The map F is called a homotopy[12] between $f_0$ and $f_1$, denoted as $f_0 \cong f_1$.*

**Definition 2** ***(Homotopic Paths)[1].*** *Two paths $f$, $g$ in $M$ are said to be equivalent if $f$ and $g$ are homotopic relative to $\{0,1\}$, denoted as $f \cong g$*

**Definition 3** ***(Homotopy Basis).*** *For a closed orientable surface $M$ with genus $g$ (i.e., a torus with $g$ handles), there are $2g$ classes of homologically independent loops, called the* homotopy basis *of the surface $M$. A homology basis consists of one loop from each class, as shown in figure 2.*

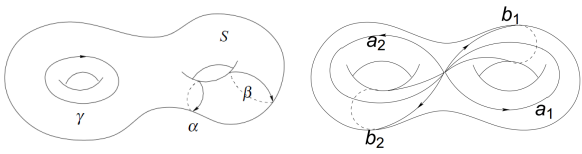


**Fig. 2.** Left: Homotopy: Curve $\alpha$ is homotopy to $\beta$, but not homotopy to $\gamma$. Right: Homotopy basis for a genus 2 surface. The number of loops $L = 2g = 4$ $\{a_1, a_2, b_1, b_2\}$, each as a representative of it's homotopy class.

### 3.2 Surface Ricci Flow

Suppose $S$ is a surface in three dimensional Euclidean space $\mathbb{R}^3$, therefore it has naturally the induced Euclidean metric $\mathbf{g}$. The Gaussian curvature is determined by the Riemannian metric $\mathbf{g}$, and satisfies the following Gauss-Bonnet theorem:

**Theorem 1 (Gauss-Bonnet Theorem).** *The total Gaussian curvature of a closed metric surface is*

$$\int_S K dA = 2\pi\chi(S),$$

*where $\chi(S)$ is the Euler number, which equals to $\chi(S) = 2 - 2g$ for closed surface with genus $g$.*

Ricci flow is a powerful curvature flow method invented by Hamilton[6] for the purpose of proving Poincaré's conjecture. Intuitively, it describes the process to deform the Riemannian metric according to curvature such that the curvature evolves like a heat diffusion process:

$$\frac{d\mathbf{g}}{dt} = -2K\mathbf{g}. \tag{1}$$

The convergence of surface Ricci flow was also proved in[6].

**Theorem 2.** *Suppose S is a closed surface with a Riemannian metric. If the total area is preserved, the surface Ricci flow will converge to a Riemannian metric of constant Gaussian curvature[6].*

Fig. 3 shows the conformal parameterization of colon surface computed by Ricci flow, figure 4 shows that conformal mapping preserves angle.

## 4 Algorithm

### 4.1 Topological De-noise

In previous work [9], the de-noise process started from the segmentation of the colon, incorporated the simple point concept in a region growing based algorithm to extract a topologically simple segmentation of the colon lumen. However, as we mentioned, the de-noise algorithm cannot guarantee the output surface is genus 0 in practice, so we developed a new efficient surface based de-noise algorithm to remove the topological

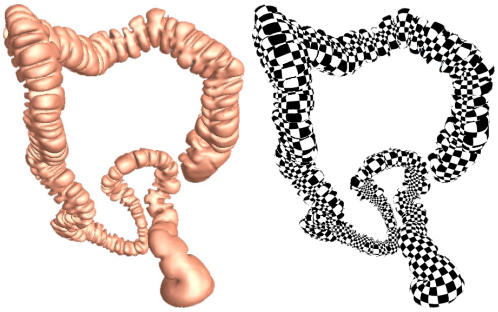

**Fig. 3.** Conformal parameterization of the colon surface

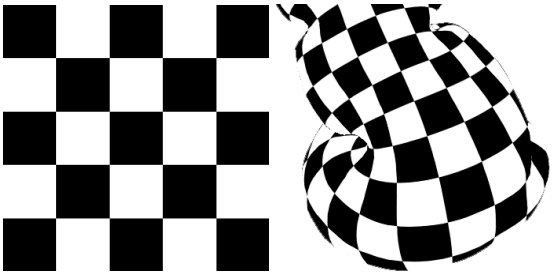

**Fig. 4.** Conformal Mapping preserves angle: the angle on the texture domain is well preserved after mapped to the surface, so the shape information of colon surface is well preserved

**Algorithm 1.** Topological De-noise Algorithm

**Input:** Surfaces $M$.
**Output:** Genus 0 surface $\bar{M}$.
1. Compute the homotopy basis $G$ of $M$ using algorithm 2.
2. For each point $p$ on homotopy basis $G$, grow a patch $P$.
3. Find the shortest homotopy loop $p_l$ starts at $p$ in patch $P$.
4. Find the shortest loop $min\{p_l\}$ among all the vertices on $G$.
5. Cut $M$ along $min\{p_l\}$ and fill the 2 holes appeared, get $\bar{M}$.
6. If $\bar{M}$ is not genus 0, goto step 1.

noise. As our method find tiny handles based on surface topology and remove them one by one, the final surface is guaranteed to be genus 0. The pipeline is like the following:

The idea of efficient topological de-noise algorithm is like following: we can compute the shortest loop goes though vertex $v$ for all the vertices in mesh $M$, then find the shortest one among them, it must be the shortest handle loop in $M$. Furthermore, all the handles of a surface must be "go around" by the homotopy basis. As a result, we just need to compute the shortest loops for vertices on the homotopy basis $G$ instead of all vertices of surface $M$, which leads to a 10 times speed up. Compared to the old voxel

based de-noise algorithm, our surface based method is much faster, and guarantees the output surface to be exactly genus 0. Fig. 5 shows a tiny handle went though by the homotopy basis.

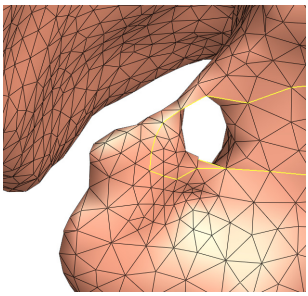

**Fig. 5.** A typical tiny hole and the homotopy basis (labeled by yellow line) goes around it

A homotopy basis at $s$ can be thought of as a homology basis where all loops meet at a common vertex $s$, called the basepoint. Erickson and Whittlesey [4] proved that a shortest homotopy basis at a point on a mesh with $n$ vertices can be computed in $O(nlogn)$ time. Fig. 6 shows the homotopy basis for genus 1 surface, algorithm 2 gives the algorithm for computing the homotopy basis:

**Algorithm 2.** Homotopy Basis Algorithm

**Input:** Surfaces $M$.
**Output:** The homotopy basis $G$ of $\bar{M}$.
1. Find the maximum spanning tree $T$ from a basepoint $s$.
2. Find a maximum spanning tree $T^*$ on the edges of the dual graph which do not cross edges in $T$.
3. Find all edges $\{e_1, e_2 ... e_{2g}\}$ which are neither in $T$ nor are crossed by edges in $T^*$.
4. Find the loops containing each $e_i$ (using $T$), these loops form the homotopy basis.

### 4.2 Discrete Ricci Flow

The computation of the conformal mapping of a triangular mesh is based on the discrete Ricci flow [11,19], as Algorithm 3 shows.

## 5 Experimental Results

CTC datasets was random selected from a database. The presented algorithm was implemented in a similar manner as the previous algorithm [9] for a fair comparison. These algorithms were executed on a PC platform of Intel Xeon X5450 3.0GHz CPU and 8.00 GB RAM. To get the maximum quality, we use the original un-simplified mesh for conformal mapping. The triangle number of the 14 datasets range from 700k to 1200k. The method in [9] can only find around half of the handles, while our method can completely remove all the handles. Table 1 shows the de-noise result comparison between

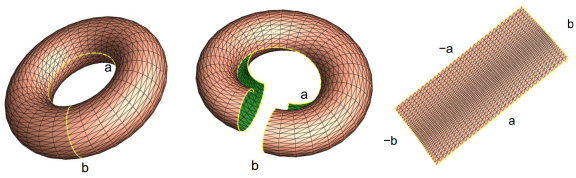


**Fig. 6.** Left: a and b are 2 homotopy basis for a genus 1 surface. Middle: The surface becomes a topological disk after cut along the it's homotopy basis. Right: Flatten the surface onto the plane.

**Algorithm 3.** Discrete Ricci Flow

**Input:** Surface $M$.

**Output:** The metric $U$ of $M$.

1. Assign a circle at vertex $v_i$ with radius $r_i$; For each edge $[v_i, v_j]$, two circles intersect at an angle $\phi_{ij}$, called edge weight.
2. The edge length $l_{ij}$ of $[v_i, v_j]$ is determined by the cosine law: $l_{ij}^2 = r_i^2 + r_j^2 - 2r_i r_j \cos\phi_{ij}$
3. The angle $\theta_i^{jk}$, related to each corner , is determined by the current edge lengths with the inverse hyperbolic cosine law.
4. Compute the discrete Gaussian curvature $K_i$ of each vertex $v_i$:

$$K_i = \begin{cases} 2\pi - \sum_{f_{ijk} \in F} \theta_i^{jk}, & \text{interior vertex} \\ \pi - \sum_{f_{ijk} \in F} \theta_i^{jk}, & \text{boundary vertex} \end{cases} \tag{2}$$

where $\theta_i^{jk}$ represents the corner angle attached to vertex $v_i$ in the face $f_{ijk}$

5. Update the radius $r_i$ of each vertex $v_i$: $r_i = r_i - \varepsilon K_i r_i$
6. Repeat the step 2 through 5, until $\|K_i\|$ of all vertices are less than a specific error tolerance.

our method and the method in [9], as well as the total running time for de-noise and conformal flattening. Notice that only 1 out of 14 case (3053S) reached genus 0 using method in [9], which means most of the data are not qualified as input of the conformal flattening algorithm, while all 14 reached genus 0 using our de-noise algorithm.

**Table 1.** De-noise Result and Time Efficiency

| Data Index | #Of mesh triangles | # NO. of handles removed by our method | # NO. of handles removed by method in [9] | # Running time (Min.) |
|---|---|---|---|---|
| 3033P | 830 K | 8 | 5 | 8.6 min |
| 3033S | 1120 K | 26 | 10 | 10.3 min |
| 3034P | 764 K | 24 | 21 | 8.1 min |
| 3034S | 800 K | 7 | 2 | 8.2 min |
| 3035S | 1060 K | 13 | 6 | 10.2 min |
| 3036P | 875 K | 13 | 8 | 8.5 min |
| 3037S | 836 K | 6 | 0 | 8.5 min |
| 3038P | 1167 K | 16 | 10 | 10.8 min |
| 3039P | 920 K | 7 | 5 | 9.4 min |
| 3039S | 1040 K | 9 | 8 | 10.0 min |
| 3041P | 902 K | 15 | 8 | 9.7 min |
| 3041S | 886 K | 4 | 1 | 9.1 min |
| 3043P | 917 K | 11 | 5 | 9.4 min |
| 3053S | 958 K | 4 | 4 | 9.6 min |

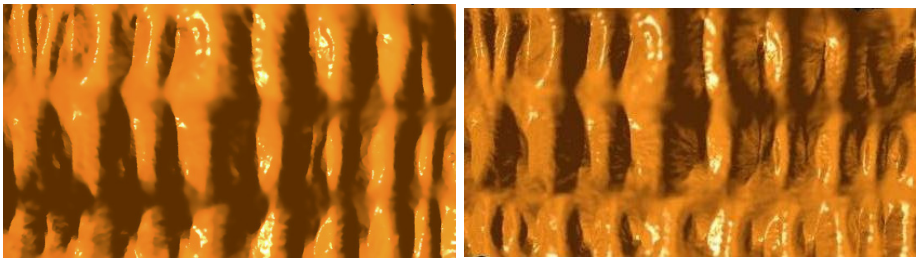

**Fig. 7.** Letf : The zoomed-in results from method in [9]. Right : The zoomed-in results from our method.

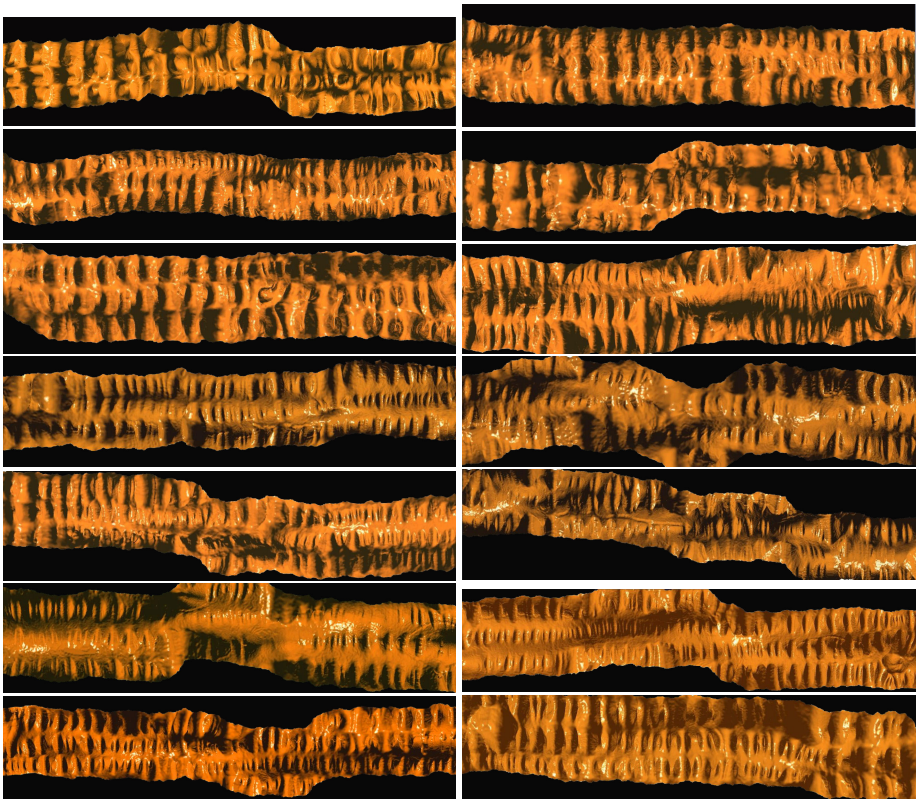

**Fig. 8.** Zoom-in flatten results of all 14 datasets

For the final colon image, figure 7 shows the zoomed in colon image of [9] and the colon image computed by our method. We can see that the image from our method is clearer and preserved more details compared with the old method. We also show zoom-in flatten results of all 14 datasets in figure 8.

## 6 Discussion

The key parts of our method is the new efficient topological de-noise algorithm. Our new topological de-noise algorithm guarantee the output to be exactly genus 0. As a result, the whole mapping process becomes much faster and more stable.

## References

1. Arbarello, E., Cornalba, M., Griffiths, P., Harris, J.: Topics in the Theory of Algebraic Curves (1938)
2. Balogh, E., Sorantin, E., Nyul, L.G., Palagyi, K., Kuba, A., Werkgartner, G., Spuller, E.: Colon unraveling based on electronic field: Recent progress and future work. In: Proceedings SPIE, pp. 713–721 (2002)
3. Bartrol, A.V., Wegenkittl, R., König, A., Gröller, E., Sorantin, E., Medgraph, T.: Virtual colon flattening (2001)
4. Erickson, J., Whittlesey, K.: Greedy optimal homotopy and homology generators. In: Proceedings of the Sixteenth Annual ACM-SIAM Symposium on Discrete Algorithms, SODA 2005, pp. 1038–1046 (2005)
5. Haker, S., Angenent, S., Kikinis, R.: Nondistorting flattening maps and the 3d visualization of colon ct images. IEEE Trans. on Medical Imaging 19, 665–670 (2000)
6. Hamilton, R.S.: The Ricci flow on surfaces. Mathematics and general relativity (Santa Cruz, CA, 1986). Contemp. Math. Amer. Math. Soc. Providence, RI 71 (1988)
7. Hong, L., Kaufman, A., Wei, Y., Viswambharan, A., Wax, M., Liang, Z.: 3d virtual colonoscopy. In: IEEE Symposium on Frontier in Biomedical Visualization, pp. 26–32 (1995)
8. Hong, L., Liang, Z., Viswambharan, A., Kaufman, A., Wax, M.: Reconstruction and visualization of 3d models of the colonic surface. IEEE Transactions on Nuclear Science, 1297–1302 (1997)
9. Hong, W., Gu, X., Qiu, F., Jin, M., Kaufman, A.: Conformal virtual colon flattening. In: ACM Symposium on Solid and Physical Modeling, pp. 85–94 (2006)
10. Hong, W., Qiu, F., Kaufman, A.: A pipeline for computer aided polyp detection. IEEE Transactions on Visualization and Computer Graphics 12, 861–868 (2006)
11. Jin, M., Kim, J., Gu, X.D.: Discrete surface ricci flow: Theory and applications. In: IMA Conference on the Mathematics of Surfaces, pp. 209–232 (2007)
12. Massey, W.: Algebraic Topology: An Introduction. Springer (1967)
13. Paik, D., Beaulieu, C., Jeffrey, R., Karadi, C.A., Napel, S.: Visualization modes for ct colonography using cylindrical and planar map projections. Journal of Computer Assisted Tomography, 179–188 (2000)
14. Pickhardt, P.J., Choi, J.R., Hwang, I., Butler, J.A., Puckett, M.L., Hildebrandt, H.A., Wong, R.K., Nugent, P.A., Mysliwiec, P.A., Schindler, W.R.: Computed tomographic virtual colonoscopy to screen for colorectal neoplasia in asymptomatic adults. New England Journal of Medicine 349(23), 2191–2200 (2003)
15. Hong, W., Qiu, F., Kaufman, A.: A pipeline for computer aided polyp detection. IEEE Transactions on Visualization and Computer Graphics, 861–868 (2006)
16. Luboldt, W., Steiner, P., Bauerfeind, P., Pelkonen, P., Debatin, J.: Detection of mass lesions with mr colonoscopy: Preliminary report. Radiology 207, 59–65 (1998)

17. Wang, S., Li, L., Cohen, H., Mankes, S., Chen, J., Liang, Z.: An em approach to map solution of segmenting tissue mixture percentages with application to ct-based virtual colonoscopy. IEEE Transactions on Medical Imaging 28, 297–310 (2009)
18. Wang, Z., Li, B., Liang, Z.: Feature-based texture display for detection of colonic polyps on flattened colon volume. In: Intl. Conf. of IEEE Engineering in Medicine and Biology (2005)
19. Zeng, W., Samaras, D., Gu, X.D.: Ricci flow for 3D shape analysis. PAMI 32(4), 662–677 (2010)